

Chapter 3

Experimental Procedures

This work can be divided into two parts including 1) spraying and collecting in-flight particles, splat and coating and 2) characterization of the particles and coatings obtained from part 1. Overall experimental procedure is shown as a block diagram in Figure 3.1.

3.1 Coating materials and substrate

3.1.1 Wire

Two types of wire used in this work were stainless steel weld wire (316LS) with diameter of 1.2 mm and stainless steel arc wire (316L) with diameter of 1.6 mm. Specification of both wires are shown in Table 3.1.

3.1.2 Substrate

Stainless steel (304) was employed as substrate for splat collection with the dimensions of 30 x 40 x 4 mm³. Stainless steel substrates were polished and cleaned prior to spraying.

For coating, mild steel was used as substrate with the dimensions of 25 x 40 x 5 mm³. Substrates were cleaned and roughened just prior to coating by grit blasting with 500 µm silicon carbide particle (Blast Master, Thailand).

3.2 Spraying procedure

Arc spray system (MEC Arcjet 95, Metallizing Equipment, India) was applied for spraying both weld wire and arc wire onto mild steel substrate with different spray parameters as shown in Table 3.2. Number of passes was kept constant for all spraying. The substrates were attached with sample holder that horizontally rotated at 70 round per second with 45 second spray time.

3.3 Collection of in-flight particles

Atomized particles or in-flight particles were collected by spraying into distilled water, which was used as collecting medium. The particle collector is shown as a schematic diagram in Figure 3.2. During spraying, the nozzle turned toward the collector containing distilled water that was covered by a 3 holes ($\varnothing = 1.2$ mm) plate.

Distance between the plate and nozzle and between the water surface and plate were 160 mm and 40 mm, respectively. Spray time and number of pass for this static position were fixed at typical 45 seconds. After spraying, suspension was then dried and the solid particles were then obtained.

3.4 Collection of splats

For splat collecting, spray gun was directly point towards a polished stainless steel substrate. The stainless steel sheet of \varnothing 2 mm 3 holes exists was placed at a distance of 160 mm from the gun. Underneath (40 mm) a sheet of 30 mm x 30 mm x 4 mm polished stainless steel was fixed and used to collect the splats. Figure 3.3 shows a schematic diagram of a splat collector.

3.5 Characterization of in-flight particle and splat

3.5.1 Size distribution

The optical microscope (Olympus, BX60M) as shown in Figure 3.4 was used to analyze shape and size of the in-flight particles, morphological aspect of splat and cross-sections of coating. Size measurement for both in-flight particles and splats were performed by optical microscope with a total number of 100 in-flight particles and 100 splats to evaluate size distributions. The average sizes and their standard deviations were calculated.

3.5.1.1 Degree of flattening

The average size of 100 in-flight particles and 100 splats as detailed in section 3.5.1 were used to calculate a degree of flattening (DF) which is the ratio of splat diameter (\varnothing_S) to the in-flight particle diameter (\varnothing_{IP})

$$DF = \frac{\phi_S}{\phi_{IP}} \quad (3.1)$$

3.5.1.2 Degree of splashing

In order to investigate splat morphology in terms of degree of splashing (DS), 100 splats images taken by an optical microscope were employed. Perimeter (P) and area (A) of each splat were measured and calculated by computer aid software (imageJ 1.34s). The degree of splashing was then calculated following the equation shown below.

$$DS = \frac{1}{4\pi} \times \frac{P^2}{A} \quad (3.2)$$

3.5.2 Morphology

Morphology of the in-flight particles and the splats were revealed by scanning electron microscope (JEOL, 5910LV, Japan) shown in Figure 3.5. As-recieved in-flight particles were sprinkled on stub for SEM evaluation. Splats collected on polished stainless steel substrates were also qualitatively characterized by scanning electron microscopy (SEM).

3.6 Characterization of coating

3.6.1 Thickness

Coating thickness was evaluated by optical microscope (Olympus, BX60M) with the 20X magnification. The thickness was randomly measured from the cross-sectioned coating for thirty points in order to obtain an average value.

3.6.2 Roughness

Surface roughness measurement of the coating was performed using a SURTRONIC 3+ supplied by Taylor Hobson as shown in Figure 3.6. A diamond stylus (10 μm diameter) traversed the coating surface with 0.3 mm/s tracing speed, 0.8 mm cut off and 4 mm traversing length. Each sample was measured by three random points in order to calculate the average surface roughness value (R_a) and standard deviation.

3.6.3 Microstructure

Scanning electron microscope (JOEL 5910LV, Japan) (Figure 3.5), was also used to characterize microstructure of coating. The microscope was operated with an accelerating voltage of 15 kV in backscattered electron mode. The coating samples were prepared by cross-sectioning perpendicular to surface of the coating using a Struers Labotom-3 wheel saw (Struers, Copenhagen, Denmark). The coating cross-sections were hot mounted in conductive phenolic mounting resin (Metkon, Conventry, UK) and the polished using 100, 200, 400, 600, 800, and 1000 grit size SiC paper and with 1.0 and 0.3 μm alumina slurry respectively.

3.6.4 Porosity and oxide

Porosity and oxide content of coating cross-sections were evaluated by image analysis (ZIEEZ, AXIO) from the cross-sections. The analysis of gray level enables to distinguish the different feature of coating microstructure. Average results were obtained by measuring porosity and oxide at ten random locations for each sample.

3.6.5 Microhardness

Vickers microhardness tester (Galileo OD) as shown in Figure 3.7 was employed for hardness measurement using 300 g load and 15 seconds dwell time. To obtain an average hardness value, microhardness measurement was performed on polished cross-sectional coating at ten random points along the central line of the coating in order.

3.7 Wear test

3.7.1 Abrasive wear test

A dry sand rubber wheel testing machine as shown in Figure 3.8 was used to evaluate the abrasive wear performance of the coatings. All coatings were examined under the same test condition. The abrasion testing was performed under the dry condition. Silica sand was employed as the abrasive particle with the particle in the range of 250-500 μm at 47 N load used. The wheel is loaded against the specimen, and rotated at 200 rpm whilst the abrasive was fed down. The abrasive was fed at a constant rate approximately 200 g/min. The wheel was set the revolution to the prescribed sliding distance (50 m).

Wear value was measured by a mass loss from the specimen. Specimen mass was determined using a Mattler Toledon (AB304-S) electronic balance with an accuracy of 0.0001g. The test sample was cleaned in acetone prior to each weighing. The mass of the specimen was measured when the test has run to the desired sliding distance and this was repeated until 250 m sliding distance had been achieved. The

wear rate quoted is the gradient of the mass loss versus sliding distance taken from the steady state regime.

3.7.2 Sliding wear test

Prior to sliding wear test, all samples were first ground with SiC paper using grit size of 100, 200, 400, 600, 800, and 1000, respectively, and then cleaned with acetone. Pin on disk tests as shown in Figure 3.9 were performed with a ISC-200 tribometer in ambient atmosphere with room temperature. For all tests, a pure WC ball with a radius of 3.15 mm was used as a counter part, and the track radius was set to 4, 6, 8 and 10 mm. The rotation speed was set to obtain a linear speed of 10 cm/s. Prior to the test, both the sample and ball were cleaned for 5 min in ethanol. All coatings were tested with a load of 100 g for 1989 revolutions. After the pin on disk tests were performed, the samples were cleaned for 5 min in ethanol. The average width of the wear tracks was obtained by measuring four points of each wear track with the optical microscope. From the width track, the volume loss of the wear track was calculated by equation 3.3. The wear rate quoted is the gradient of the volume loss versus sliding distance.

$$\text{Volume loss (mm}^3\text{)} = \frac{\pi(\text{wear track radius, mm}) (\text{track width, mm})^3}{6(\text{sphere radius, mm})} \quad (3.3)$$

Table 3.1 Wire nominal specifications

Types of wire	Chemical composition (% wt/wt)									
	C	Si	Mn	P	S	Cr	Mo	Ni	Cu	N
Stainless steel weld wire (ER316LS), ϕ 1.2 mm, Lincoln Electric Company, U.S.A.	0.024	0.82	2.00	0.025	0.007	18.50	2.56	13.68	0.16	0.037
Stainless steel arc wire (ER 316L), ϕ 1.6 mm, Flame Spray Technologies, U.S.A.	0.013	0.81	1.60	0.015	0.01	18.30	2.52	12.2	0.09	0.043

Table 3.2 Arc spray conditions

Parameters	Designation	Voltage	Spray distance	Air pressure
		(V)	(mm)	(kPa)
Weld wire (varied)	C ₁	26	200	420
	C ₂	26	200	520
	C ₃	26	300	420
	C ₄	26	300	520
Arc wire (recommended)	C ₅	30	150	520

Note : weld wire spraying conditions were varied due to weld wire is normally used for welding process, no recommendation for arc process previously reported.

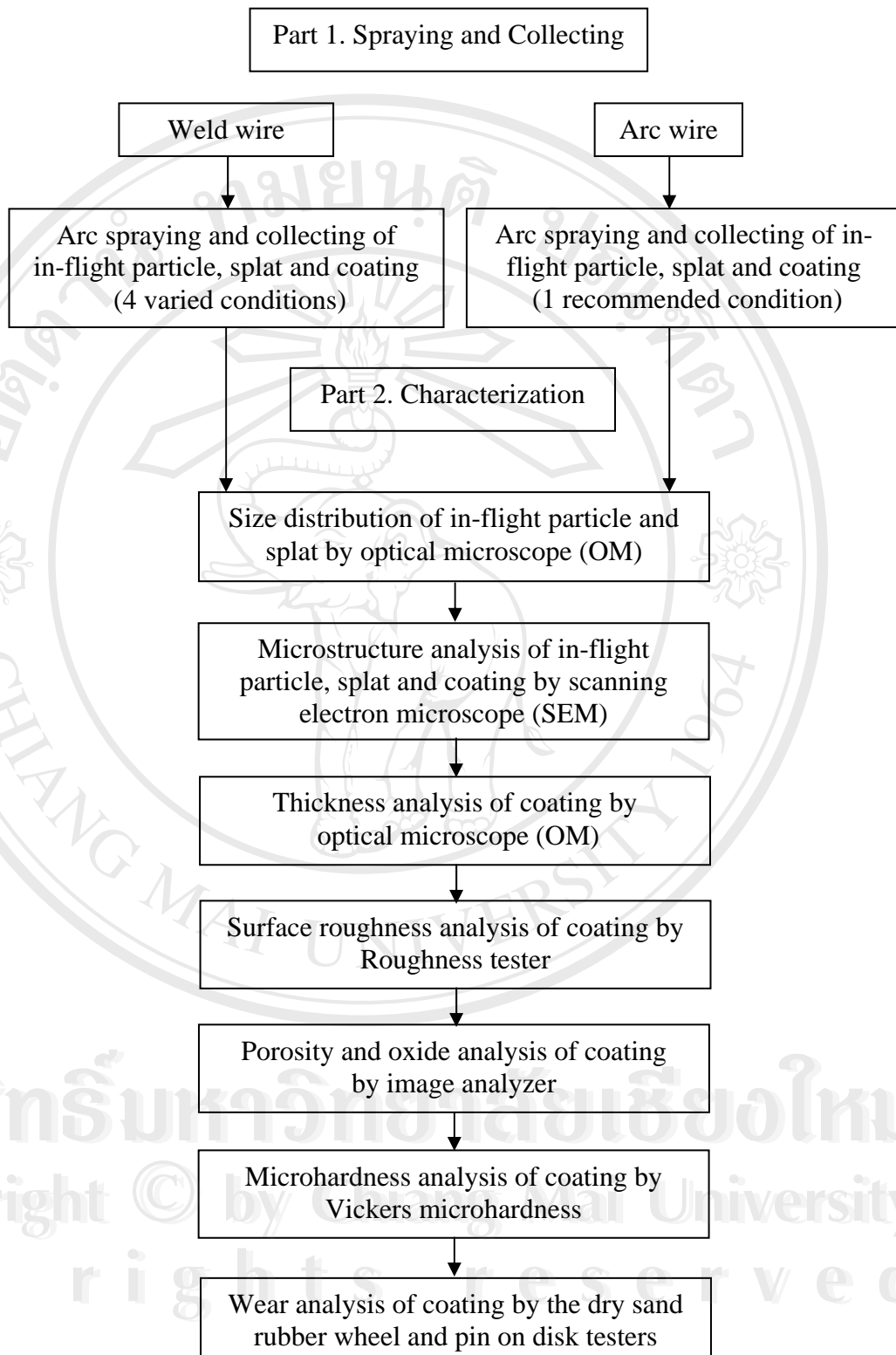


Figure 3.1 Diagram shows the overall experimental procedure.

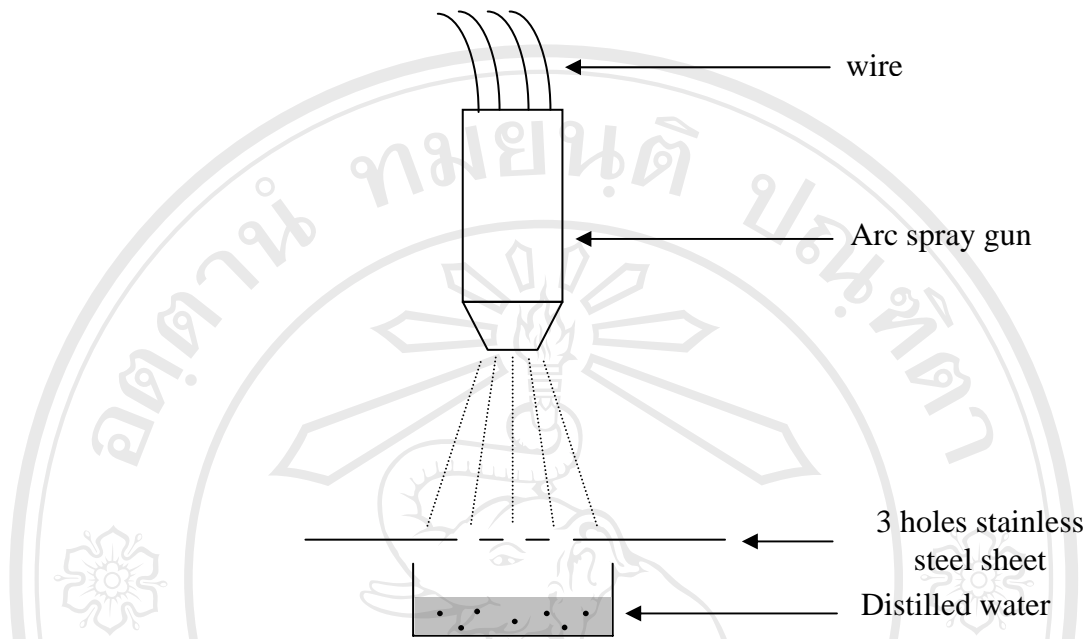


Figure 3.2 An in-flight particle collector

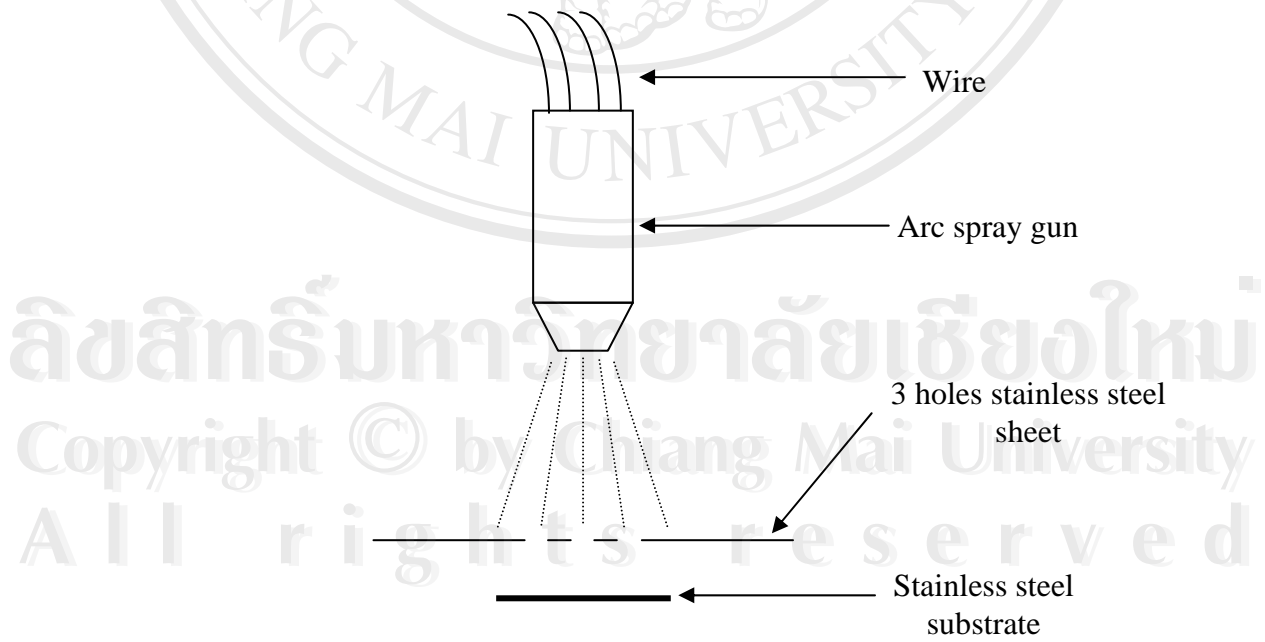


Figure 3.3 A splat collector



Figure 3.4 Optical microscope (OM)



Figure 3.5 Scanning electron microscope (SEM)



Figure 3.6 Surface profilometer



Figure 3.7 A Vickers microhardness tester



Figure 3.8 A dry sand rubber wheel testing machine



Figure 3.9 A pin on disk sliding wear tester